Indian Journal of Chemistry
Vol. 56A, December 2017, pp. 1302-1309

Thionine-functionalized graphene oxide nanosheet as an efficient electrocatalyst for NADH oxidation and H_2O_2 reduction

Ali A Ensafi*, Navid Zandi-Atashbar, Zeynab Ahmadi Sarsahra & Behzad Rezaei

Department of Chemistry, Isfahan University of Technology, Isfahan 84156-83111, Iran
Email: ensafi@cc.iut.ac.ir/ensafi@yahoo.com/aaensafi@gmail.com

Received 24 September 2017; revised and accepted 29 November 2017

Thionine-functionalized graphene oxide (Th-GO) has been successfully prepared for use as an efficient electrocatalyst in the electrochemical detection of hydrogen peroxide and nicotinamide adenine dinucleotide (NADH), and subsequently characterized by FT-IR spectroscopy, X-ray diffraction, transmission and scanning electron microscopy, and electrochemical methods. Electrochemical studies reveal that the carbon paste electrode modified with Th-GO decreases the working potentials to 0.24 V and 0.00 V towards oxidation of NADH and reduction of H_2O_2, respectively. Two linear ranges of 2.0–200 μmol L^{-1} and 200–500 μmol L^{-1} and a detection limit of 0.43 μmol L^{-1} have been obtained for NADH analysis. These quantitative data for H_2O_2 determination are 2.0–3500 μmol L^{-1} and 1.3 μmol L^{-1} respectively. Th-GO/CPE shows satisfactory results in terms of repeatability, reproducibility, and selectivity towards NADH and H_2O_2 analysis in both buffer and real sample.

Keywords: Electrocatalysts, Electrodes, Modified electrodes, Functionalised electrodes, Thionine-functionalized graphene oxide, Graphene oxide, Hydrogen peroxide, Nicotinamide adenine dinucleotide, Chronoamperometry

Hydrogen peroxide, a source of radical oxygen, is a by-product of oxidative metabolic pathways catalyzed by a large number of oxidase enzymes[1,2]. Hydrogen peroxide and its derivatives play important roles in the manufacture of many foods, clinical, and bleaching products.[1] Moreover, it is used as an oxidizing agent in cosmetic products.[3] H_2O_2 measurement is, therefore, essential in many industrial situations. Several methods have been reported for the analysis of H_2O_2 that include spectrometry, titrimetry, chemiluminescence, and electrochemical techniques.[4-8] Among the detecting techniques, electrochemical sensors have been developed because of their operational simplicity, low cost, high sensitivity, high selectivity, and the modifiability of the electrode with newly synthesized materials.[9-11] Electrochemical detection of H_2O_2 based on enzymes is a method commonly used due to its high sensitivity and selectivity. However, application of such sensors is limited by their operating conditions such as pH and temperature as well as such inherent drawbacks as high cost and complicated preparation procedures.[12] These observations have led to a growing interest in non-enzymatic H_2O_2 sensors based on new materials as good candidates for H_2O_2 determination.[1]

The bio-species nicotinamide adenine dinucleotide (NADH) and its cation (NAD^+) are present in vivo not only in eukaryotic and prokaryotic organisms[13] but also as the main coenzyme in the human body. It may naturally form in any living cell through the digestion of consumed food. As a coenzyme, NADH is involved in many metabolic reactions such as those that stimulate brain functions, provide energy for the immune system, and repair the DNA system.[14,15]

A variety of methods have been employed for the analysis of NADH; these include colorimetry, fluorometry, and liquid chromatography.[16-18] Despite their high sensitivity in monitoring NADH, they have drawbacks such as complex preparation, complicated operation, and high cost due to the expensive reagents used.[19] Electrooxidation of NADH at an overvoltage leads to irreversible reactions of NAD^+ yielding products that are adsorbed on the electrode surface. The resulting electrode contamination gives rise to the presence of background currents that cause interference in the analysis of real samples.[20] Hence, it is essential to decrease the overpotential by modifying the electrode with new mediators.

Graphene oxide (GO) is a commonly employed chemical derivation of graphene. Its numerous oxygen-containing functional groups offer a large number of active sites for further chemical modification by organic and non-organic binders. The surface of graphene can be thus modified using diazonium chemistry, in which functionalization is performed by dyes.[21-23] The dyes are utilized as redox mediators in electrocatalytic reactions because of their high electron

transferring capacity, low cost, and water solubility.[23] Moreover, the presence of diazonium dyes protects the graphene nanosheets from agglomeration.

In this work, graphene oxide (GO) was functionalized by thionine (Th) using diazonium reaction and the Th-GO thus prepared was characterized by different methods. Th-GO was then used as an electrocatalyst in a carbon paste electrode (CPE) to detect NADH and H_2O_2 by electrochemical techniques such as cyclic voltammetry and hydrodynamic chronoamperometry. The electro-catalytic effects of thionine towards oxidation of NADH and reduction of H_2O_2 were observed when Th-GO/CPE was employed. Moreover, monitoring NADH and H_2O_2 by Th-GO/CPE was found to be repeatable and reproducible yielding selective results. It also exhibited a satisfactory performance in the analysis of real samples with very low detection limits.

Materials and Methods

Hydrogen peroxide, nicotinamide adenine dinucleotide (NADH) (99%) and thionine were purchased from Sigma-Aldrich. Graphite powder and all other reagents, at analytical grades, were provided by Merck and used without further purification. Phosphate solution was used as an electrolyte. The pH of the phosphate solution (PBS) was adjusted by adding NaOH solution (3.0 mol L^{-1}) to 0.10 mol L^{-1} of H_3PO_4 solution.

All the voltammetric and amperometric examinations were conducted using an electrochemical analyzer (Autolab, PGSTAT-30 potentiostat-galvanostat) equipped with a micro–computer to record the electrochemical data. Data processing was accomplished using the GPSE computerize software. Electrochemical studies were performed using a conventional three-electrode system in which a platinum rod, a saturated Ag/AgCl electrode, and a thionine-functionalized graphene oxide carbon paste electrode (Th-GO/CPE) served as the auxiliary, the reference, and the working electrodes, respectively. The pH of each solution was adjusted using a pH-meter (Corning, Model 140) with a double junction glass electrode. For each electrode, electron transfer resistance was measured via electrochemical impedance spectroscopy (EIS). All EIS studies were accomplished in the frequency range 0.01 Hz to 100 kHz at amplitude wave potentials of 10 mV and 0.20 V as the applied potentials in a 10.0 mmol L^{-1} $Fe(CN)_6^{3-/4-}$ and 0.10 mol L^{-1} KNO_3 solution used as the probe. XRD analyses were conducted using a Bruker D8/Advance X-ray diffractometer with Cu-K_α radiation. FT-IR spectra were recorded on a Jasco FT-IR/680 plus at 400–4000 cm^{-1} as KBr pellets. Field emission scanning electron microscopic (FE-SEM) images were recorded using an XL-30 ESEM at an accelerating voltage of 20 kV. TEM images were prepared using a transmission electron microscope (model CM30 TEM, Philips, The Netherlands) operated at 200 kV.

Preparation and functionalization of graphene oxide

Graphene oxide was prepared according to the modified Hummer method.[23] Briefly, 3.5 g of graphite powder, 12.0 mL of conc. H_2SO_4, 2.5 g of $K_2S_2O_8$, and 2.50 g of P_2O_5 were mixed and refluxed at 80 °C for 4.5 h. The mixture was then diluted with distilled water, filtered, thoroughly rinsed, and finally dried under vacuum. Pre-oxidized graphite powder was taken in 120 mL of conc. H_2SO_4. To the mixture prepared above, was added 15.0 g $KMnO_4$ under gentle stirring to cool to a temperature below 20 °C. The mixture was stirred at 35 °C for 2 h before it was diluted with water to 250 mL. Subsequently, it was further diluted up to 950 mL with water and stirred for another 2 h. The final mixture was mixed with 20 mL H_2O_2 (30%), filtered, and washed with 1.0 L HCl solution (1:10 *v*/*v*) while being repeatedly rinsed with distilled water till the pH of the filtrate to became neutral. Finally, graphene oxide (GO) was obtained by dispersing the resulting material in distilled water in an ultrasonic bath for 1 h.[23]

Functionalization of graphene oxide with thionine was carried out using the diazonium reaction. First, 250 mg of thionine was dissolved in 12 mL of HCl (18%) and 250 mg of graphene oxide and 0.50 g of Fe powder were added to the solution. Then, the mixture was treated with 25 mg $NaNO_2$ in an ice bath and vigorously stirred for 12 h. The functionalized product (Th-GO) was filtered and thoroughly washed with distilled water until the pH of the filtrate was neutral.[23]

Preparation of modified carbon paste electrodes

To prepare modified CPE, 0.35 g of paraffin oil, 0.45 g of graphite powder, and 0.20 g of Th-GO were mixed in an agate mortar to obtain a homogenous carbon paste. A copper wire was then inserted into the paste to conduct an electrical current between the solution medium and the electrode. The unmodified electrode was similarly prepared by mixing only 0.65 g of graphite powder with 0.35 g of paraffin oil. The CPEs were polished on a piece of weighing paper to expose new, usable, and smooth surfaces.

Results and Discussion

Characterization of the prepared Th-GO

The preparation of Th-GO was characterized by XRD, FT-IR, and electron microscopic techniques of FE-SEM and TEM as well as cyclic voltammetry.

FT-IR was used to investigate the step by step preparation of Th-GO as follows: (a) graphene oxide, (b) Th-GO treated with Fe, (c) in the absence of Fe (Fig. 1(a)). Comparison of the spectra in Fig. 1a (curves 2 & 3) reveals that the presence of Fe powder during the synthesis of Th-GO facilitates Th immobilization on GO via the diazonium reaction. The corresponding infrared bands in the spectrum of thionine acetate are also shown in curve (4) of Fig. 1(a). The formation of GO was confirmed by the bands at 3300–3600, 1600, and 1100 cm^{-1} corresponding to the stretching vibration of OH, the aromatic bond of C=C, and the stretching vibration of C–O, respectively. In the spectrum of Th-GO, several new peaks appeared that are not present in the corresponding spectrum of GO; for instance, the absorption band of 1580 cm^{-1} due to the bending vibration of N–H. Comparison of the spectra indicates that this peak is more intense in the presence of iron during the synthesis of Th-GO. This is the result of more effective functionalizing of thionine on GO by the catalytic effect of iron powder.

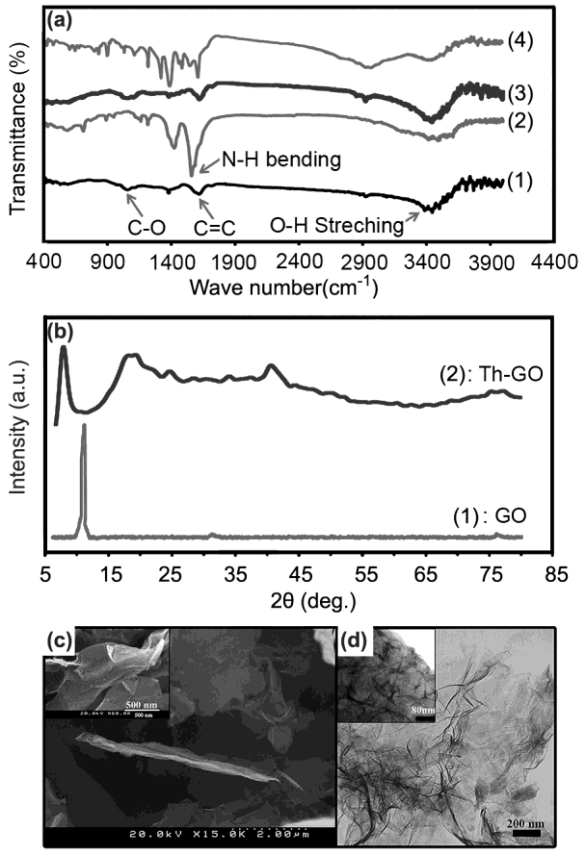

Fig. 1 — (a) FT-IR spectra of GO (1), Th-GO (in the presence of iron powder in the synthesis pathway) (2), Th-GO (in the absence of iron powder in the synthesis pathway) (3), and thionine acetate (4). (b) XRD patterns of GO (1), and, Th-GO (2). (c) FE-SEM image of Th-GO. (d) TEM image of Th-GO.

The XRD patterns of graphene oxide and thionine-functionalized GO (f) are shown in Fig. 1(b). The diffraction peak located at 10.00° is attributed to the graphene oxide.[24] The calculation of the sheet distances at 2θ = 23° revealed that graphene functionalization led to increased separation of the graphene sheets from 3 Å to 4.1 Å due to the insertion of thionine molecules between the graphene sheets.

The surface morphologies of the graphene oxide nanosheets functionalized with thionine can be seen in the microscopic images of FE-SEM (Fig. 1(c)) and TEM (Fig. 1(d)). As can be seen, graphene oxide nanosheets are adequately separated from each other by a thionine interlayer.

Th-GO/CPE was examined in PBS media at different pH levels (2.0–9.0) using cyclic voltammetry at a scan rate of 25 mV s^{-1}. As pH increased toward an alkaline medium, the cathodic peaks were located at more negative potentials (Fig. 2a). These values showed that thionine could be reduced in a more facile fashion when acidic solutions were used. Accordingly, the relationship between the cathodic peak potential and the solution pH was obtained as a regression equation E (V) = –0.056pH + 0.322, which agrees with the equation $E = E_0 - (0.0592\ mpH/n)$ for a proton-to-electron ratio equal to unity.

For further electrochemical characterization, electrochemical impedance spectroscopy (EIS) was used to study CPE, GO/CPE, and Th-GO/CPE with respect to their charge transfer resistance in the frequency range of 100 kHz to 10 mHz in 10.0 mmol L^{-1} $Fe(CN)_6^{3-/4-}$ and 0.10 mol L^{-1} KNO_3 solution used as the probe (Fig. 2(b)). It can be seen that a well-defined semi-circle obtained at higher frequencies at the CPE due to the charge transfer process at the electrode-electrolyte interface (Fig. 2(b), curve 1). On the other hand, at the graphene modified CPE, the charge transfer resistance value decreased distinctively, indicating that graphene oxide had accelerated electron transfer between the probe and the electrode (Fig. 2(b), curve 2). For Th-GO/CPE, incorporation of Th in GO/CPE decreased the charge transfer resistance compared to the unmodified CPE

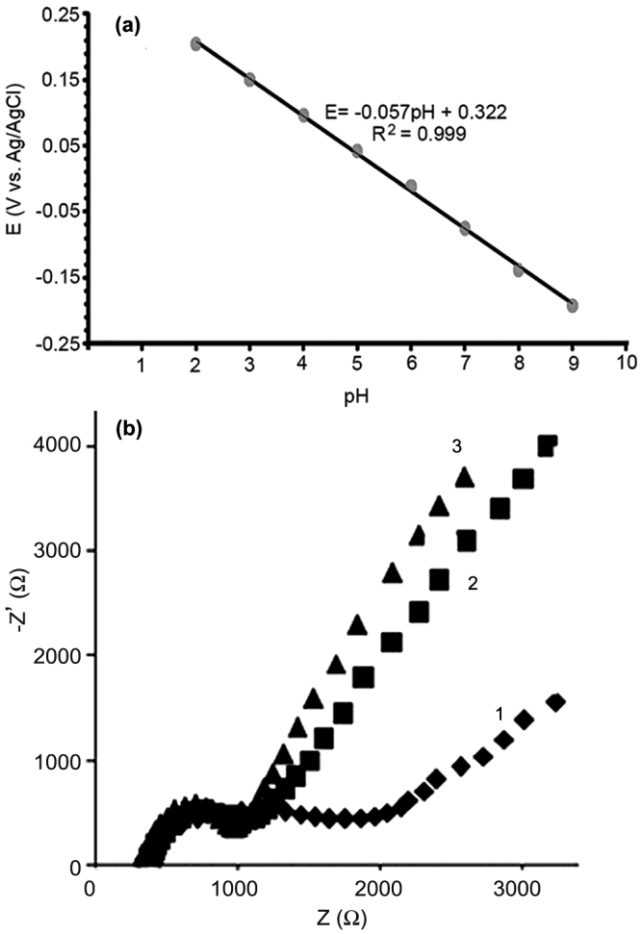

Fig. 2 — (a) Plot of the cathodic potential of Th-GO/CPE in varying pH, in the potential window of –0.90 to 0.90 V (versus Ag/AgCl) at scan rate of 25 mV s^{-1}. (b) Nyquist plots of CPE (1), GO/CPE (2) and Th-GO/CPE (3) in 10 mmol L^{-1} in 0.10 mol L^{-1} KNO_3 and 10 mmol L^{-1} $Fe(CN)_6^{3-,4-}$ in the frequency range of 100 kHz to 10 MHz.

whose charge transfer resistance was slightly higher than that of GO/CPE. The reduced charge transfer resistance at the Th-GO/CPE obviously illustrated successful functionalization of graphene oxide sheets because of the semiconductive property of Th (Fig. 2(b), curve 3).

Electrocatalytic effect of Th-GO/CPE towards oxidation of NADH and reduction of H_2O_2

The prepared modified electrode was studied to analyze NADH and H_2O_2 separately. First, the effect of pH on the peak current of the electrode toward the oxidation of NADH and reduction of H_2O_2 was studied for different pH values. Analysis of NADH and H_2O_2 in PBS solutions with different pH levels from 2.0 to 9.0 (0.1 mol L^{-1}) revealed that the modified electrode exhibited its highest sensitivity toward both NADH (Fig. 3a) and H_2O_2 (Fig. 3b) at

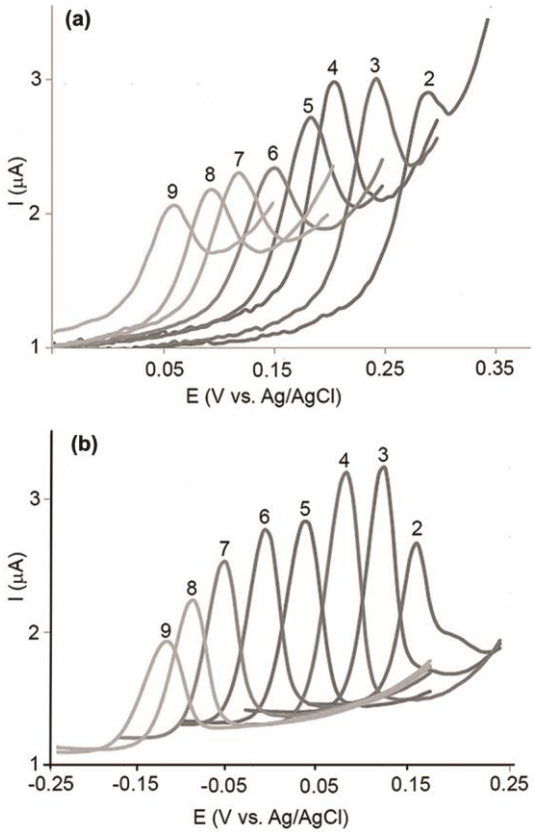

Fig. 3 — Influence of pH on peak current of (a) oxidation of NADH, and, (b) reduction of H_2O_2. [pH: 2-9].

pH 3.0. Accordingly, cyclic voltammograms in the absence and presence of NADH (20.0 μmol L^{-1}) in PBS (0.1 mol L^{-1}, pH 3.0) were recorded at the surface of unmodified CPE (Fig. 4(a), curves 1 & 2) and at Th-GO/CPE (Fig. 4(a), curves 3 & 4), respectively. In the same way, the electrocatalytic effects of the electrode were studied in the absence and presence of 0.2 mmol L^{-1} H_2O_2 at the unmodified CPE and at TH-GO/CPE (Fig. 4). According to Fig. 4, the CVs at the unmodified electrode show no significantly increasing signals in the presence of NADH or H_2O_2 when compared with the analyses conducted at the surface of the modified Th-GO/CPE. In addition to increases in the signals, more satisfactory potentials of NADH oxidation and H_2O_2 were observed at the modified electrode than at the unmodified CPE. This can be explained by the electrocatalytic effect of the modifier due to the more facile electron transfer of Th-GO/CPE.

To study the mass transfer mechanism, the scan rate of the potential on the sensor signal was investigated in the range of 10–500 mV s^{-1} by cyclic voltammetry (Fig. 5a). The linear correlation between the oxidation current in the presence of NADH

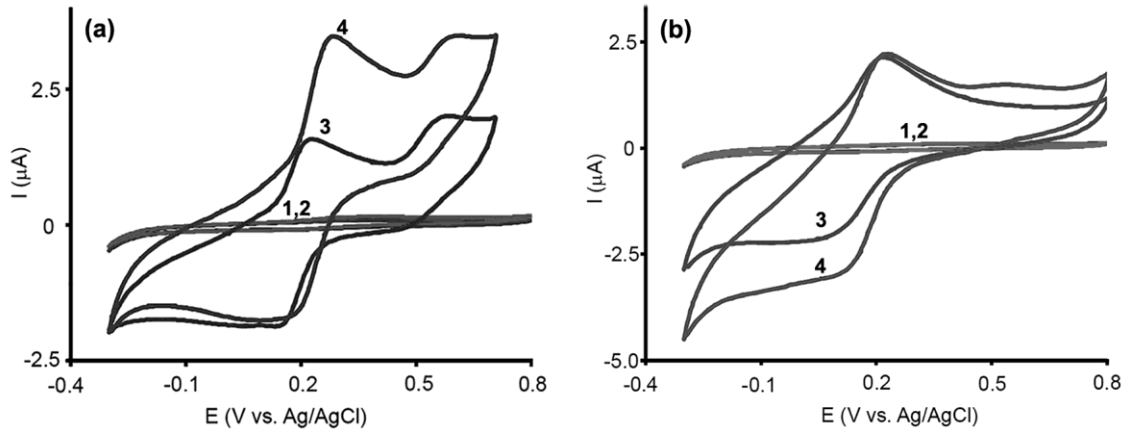

Fig. 4 — (a) Cyclic voltammograms at unmodified CPE in the absence (1) and presence of 20 μmol L^{-1} NADH (2), and at Th-GO/CPE in the absence (3) and presence of 20.0 μmol L^{-1} NADH (4). (b) Cyclic voltammograms at unmodified CPE in the absence (1) and presence of 0.20 mmol L^{-1} H_2O_2 (2), and at Th-GO/CPE in the absence (3) and presence of 0.20 mmol L^{-1} H_2O_2 (4). [Cond.: in PBS (0.1 mol L^{-1}, pH 3.0); scan rate of 25 mV s^{-1}].

(Fig. 5b) and the reduction current in the presence of H_2O_2 (Fig. 5c) versus the square root of scan rate revealed that the electrochemical reactions at Th-GO/CPE were controlled by diffusion, as regressed in i (μA) = $+1.614v^{1/2}$ ($mV^{1/2}$ $s^{-1/2}$) – 3.31 and i (μA) = $–0.695v^{1/2}$ ($mV^{1/2}$ $s^{-1/2}$) + 1.86, respectively.

Chronoamperometric responses to NADH and H_2O_2

NADH and H_2O_2 were separately analyzed in PBS (0.1 mol L^{-1}, pH 3) by successive addition of the analytes. The applied potential was varied in the range of 0.20–0.26 V (versus Ag/AgCl) for the oxidation of NADH as shown in Fig. 6(a). The reduction of H_2O_2 at different potentials (+0.10 to –0.05 V versus Ag/AgCl) was also evaluated as in Fig. 6(b). It was found that increasing oxidation potential up to an applied potential of 0.24 V led to the higher sensitivity of the electrode . Although the same results were obtained when higher cathodic potentials were applied for the efficient reduction of H_2O_2, there was non-significant increase in the amperometric signals compared to zero potential. A potential of 0.00 was, therefore, selected for further investigation of H_2O_2 analysis.

When, the Th-GO content of the CPE was varied from 2.0–20 wt%, it was observed that the higher the Th-GO content of the electrode, the more intense is the amperometric signals for the oxidation and reduction of NADH and H_2O_2 (Fig. 6 (c & d). The easier electron transfer in the oxidation of NADH and reduction of H_2O_2 may be due to the presence of the modifier Th-GO. A higher Th-GO content could have resulted in a tougher paste, and hence a

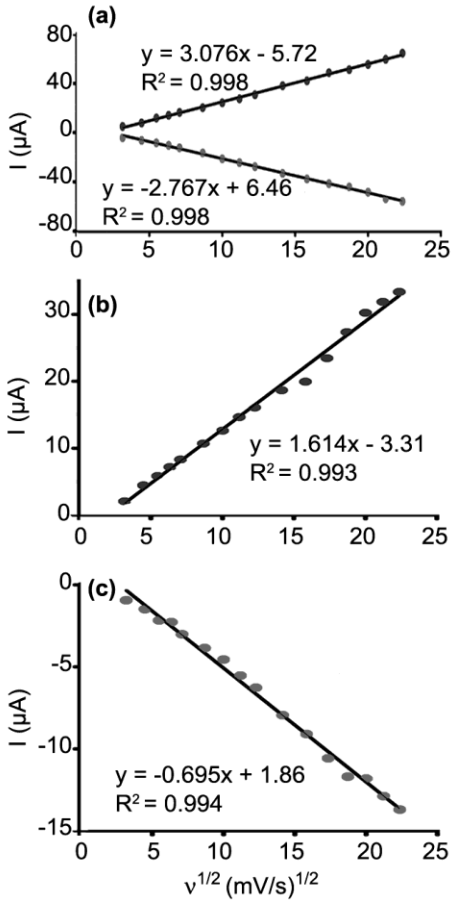

Fig. 5 — Plot of the anodic and cathodic currents of Th-GO/CPE versus the square root of the scan rate in the range of 10–500 mV s^{-1} in (a) PBS (0.1 mol L^{-1}, pH 3.0), (b) PBS (0.1 mol L^{-1}, pH 3.0) in the presence of 20.0 μmol L^{-1} NADH, and, (c) PBS (0.1 mol L^{-1}, pH 3.0) in the presence of 0.20 mmol L^{-1} H_2O_2.

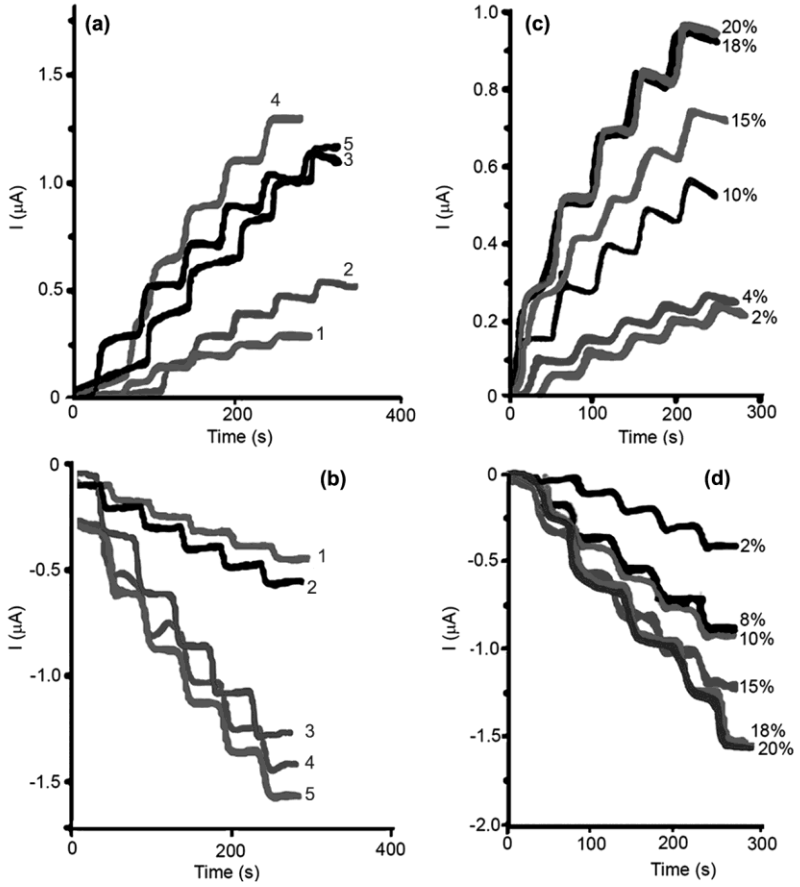

Fig. 6 — (a) Current-time response of Th-GO/CPE with successive addition of 20.0 μmol L^{-1} NADH versus Ag/AgCl. [Appl. potential (V): 0.20 (1), 0.23 (2), 0.24 (3), 0.25 (4), 0.26. (b) Current-time response of Th-GO/CPE with successive addition of 0.20 mmol L^{-1} H_2O_2 versus Ag/AgCl. [Appl. potential (V): 0.10 (1), 0.05 (2), 0.00 (3), –0.01 (4), –0.05 (5). (c) Weight percentages of the modifier from 2.0–20.0 wt% for analysis of NADH in conc. range of 20.0–200.0 μmol L^{-1}. (d) Weight percentages of the modifier from 2–20 wt% for analysis of H_2O_2 in conc. range of 0.2–2.0 mmol L^{-1}. [Cond.: in PBS (0.1 mol L^{-1}, pH 3.0 at rotating disk electrode with rotating rate of 1500 rpm].

non-renewable surface for further analysis. Thus, a Th-GO content of 20 wt% was selected as the optimized modifier content.

Under the optimum conditions, calibration curves were plotted by successive addition of NADH (at +0.24 V versus Ag/AgCl) and H_2O_2 (at 0.00 V versus Ag/AgCl) to 0.1 mol L^{-1} PBS by hydrodynamic amperometry at Th-GO/CPE. Continuous injections of NADH and H_2O_2 solutions led to increasing anodic and cathodic currents at response times of less than 5 s. As shown in Fig. 7, Th-GO/CPE presented two linear ranges versus NADH concentration: 2.0–200.0 μmol L^{-1} and 200.0–500.0 μmol L^{-1} NADH with linear regressions of i (μA) = +0.0195C (μM) + 0.643 (R^2 = 0.997) and i (μA) = +0.0092C (μM) + 2.6334 (R^2 = 0.995). A linear range versus H_2O_2 concentration of 2.0–3500.0 μmol L^{-1} H_2O_2 was also observed with the linear regression of i (μA) = –0.0018C (μM) – 0.127 (R^2 = 0.999). The two linear ranges of amperometric responses versus NADH addition may be due to the adsorption of the intermediate, or, the low concentration of NADH gives rise to amperometric signals from the oxidation of diffusive NADH, and higher levels of NADH led to the decline in the slope of the calibration curve because of the adsorption of the NADH oxidation product, which decreased the number of active sites of thionine-functionalized graphene oxide nanosheets and hindered NADH diffusion into the electrode surface.

The detection limits were calculated (= 3s/m, where s is the standard deviation and m is the slope of the calibration curve) as 0.43 μmol L^{-1} NADH and 1.3 μmol L^{-1} H_2O_2. The performance of the present sensor was compared with that of other reported NADH and H_2O_2 sensors (Table 1). It is clear that the detection limits, linear dynamic ranges, and the applied potential of the prepared sensor are comparable to those obtained by other modified electrodes.

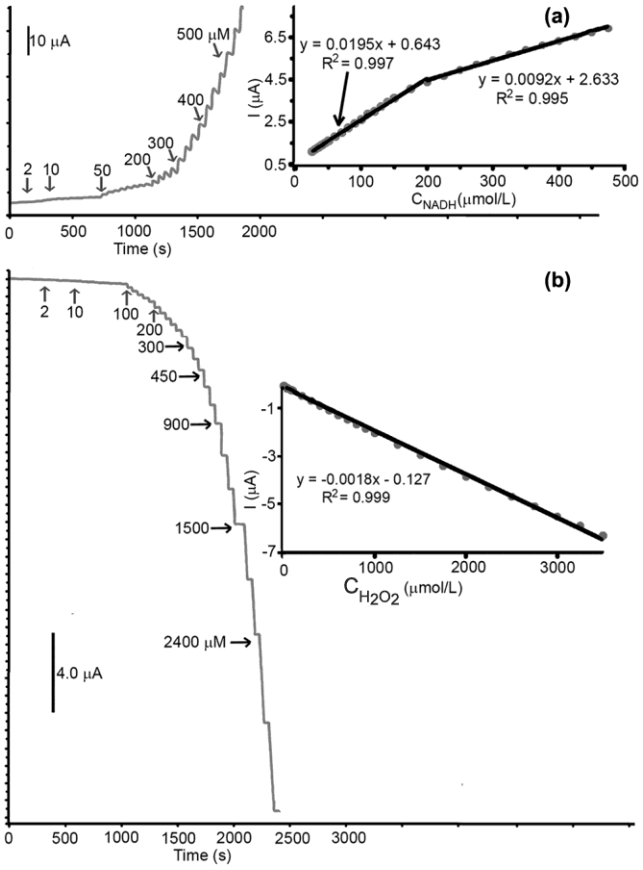

Fig. 7 — Current-time (*i*-*t*) curves of modified electrode (Th-GO/CPE) on successive addition of (a) NADH and (b) H_2O_2, at the surface of the electrode with working applied potentials of 0.24 V and 0.00 V (versus Ag/AgCl), respectively. [Insets: Respective calibration curves].

Repeatability, reproducibility, and selectivity for NADH and H_2O_2 analyses

The repeatability of the sensor was studied by 10 continuous additions of 5.0 μmol L^{-1} NADH and 25.0 μmol L^{-1} H_2O_2 to evaluate the relative standard deviations (RSD) obtained from successive increase in amperometric signals to obtain a value of 4.1% for the oxidation of NADH and 3.8% for the reduction of H_2O_2. In addition, the reproducibility of the sensor was examined using five separate sensors. The RSD values of the modified electrode obtained for the determination of NADH and H_2O_2 are 6.2% and 5.5%, respectively.

Four interference species, viz., uric acid, ascorbic acid, dopamine, and glucose, were separately studied in the presence of NADH and H_2O_2 under the optimum conditions. The interference was determined as the identical concentration of an interfering species that could decrease or increase the electrode signal towards the analyte by a value greater than that predicted by the Student's t-test. The data obtained exhibited no significant effects on the amperometric signals resulting from the presence of NADH and H_2O_2.

Real sample analysis

To demonstrate the practical applicability of Th-GO/CPE for the determination of H_2O_2 in real samples, hair color oxidant was analysed. The sample was prepared by diluting 53.0 mg of hair color oxidant to 5.0 mL with distilled water. Amperometric measurements were made

Table 1 — Comparison of the analytical performance of various electrodes in electrochemical sensing of H_2O_2 and NADH

Sensor	Electrode	Detection limit (μmol L^{-1})	Linear range (μmol L^{-1})	Appl. potential (V)	Ref.
NADH sensor	PNR-FAD-MWCNT/GCE	1.3	1.3–933.3	0.05	25
	Acid-microwaved CNTs/GCE	2.0	10–100	–0.05	26
	Co_3O_4/CPE	4.25	10–100	0.25	27
	NiO/CPE	4	5–500	0.40	28
	$CoFe_2O_4$/EGO/GCE	0.38	0.5–100	0.45	2
	Th-GO/CPE	0.43	2.0–200 & 200–500	0.24	This work
H_2O_2 sensor	SiO_2-pro-NH_2/CPE	0.85	5.14–1250	–0.30	1
	$CoFe_2O_4$/EGO/GCE	0.5	0.9–900	–0.15	2
	Au/SnO_2-MTs/GCE	0.6	10.0–1000	–0.30	5
	MnO_2 nanowires/GPE	10	100–45000	–0.50	6
	PPy/Mn/GCE	2.12	5.0–900	–0.20	9
	CuS/GCE	1.1	10.0–1900	–0.65	10
	Nonporous PdFe/GCE	2.1	500–6000	0.30	11
	Th-GO/CPE	1.3	2.0–3500	0.0	This work

according to the standard addition method. For this purpose, 2.0 mL of the oxidant solution was added to 38.0 mL of PBS (0.1 mol L^{-1}, pH 3.0) and the current response was recorded at 0.24 V. The H_2O_2 content was estimated as 15.0±0.2 mmol L^{-1} (10.0 wt%). To verify the accuracy of the amperometric results, the real sample was independently measured using the classical potassium permanganate titration method to obtain H_2O_2 concentration of 15.6±0.4 mmol L^{-1}. This value is in good agreement with that obtained from the proposed electrochemical sensor.

Conclusions

Graphene oxide was successfully functionalized with thionine and used to modify the carbon paste electrode. The Th-GO/CPE was characterized using FT-IR spectroscopy, XRD patterns, microscopic monitoring of TEM and SEM, and the electrochemical technique of cyclic voltammetry. The prepared sensor was employed for the oxidation of NADH and reduction of H_2O_2 with increasing currents at low overpotentials hydrodynamic chronoamperometry. The experimental conditions were optimized as pH 3.0 (PBS, 0.1 mol L^{-1}), 20 wt% of the modifier, and a working potential of 0.24 V for the oxidation of NADH and 0.00 V for the reduction of H_2O_2. The results showed that modification of the electrode facilitated the electron transfer because of thionine bonding to graphene oxide. The Th-GO/CPE was used as a repeatable, reproducible, and selective sensor towards NADH and H_2O_2 measurements. Th-GO/CPE presented relatively good limits of detection for NADH and H_2O_2 determination. Finally, analysis of a real sample yielded results close to those obtained from classical titration of H_2O_2 by potassium permanganate.

References

1 Ensafi A A, Zandi-Atashbar N, Ghiaci M, Taghizadeh M & Rezaei B, *Mater Sci Eng C*, 47 (2015) 290.

2 Ensafi A A, Alinajafi H A, Jafari-Asl M, Rezaei B & Ghazaei F, *Mater Sci Eng C*, 60 (2016) 276.

3 Packianathan N & Karumbayaram S, *J Pharm Sci Res*, 2 (2010) 648.

4 Vogel A I, *Textbook of Quantitative Chemical Analysis*, (Longman, UK) 1989.

5 Liu S, Yu B, Li F, Ji Y & Zhang T, *Electrochim Acta*, 141 (2014) 161.

6 Dong S, Xi J, Wu Y, Liu H, Fu C, Liu H & Xiao F, *Anal Chim Acta*, 853 (2015) 200.

7 Xu G & Dong S, *Electroanalysis*, 11 (1999) 1180.

8 Chen X, Su B, Cai Z, Chen X & Oyama M, *Sense Actuators B Chem*, 201 (2014) 286.

9 Mahmoudian M R, Alias Y, Basirun W J, Moradi Golsheikh A & Jamali-Sheini F, *Mater Chem Phys*, 141 (2013) 298.

10 Kumar Dutta A, Das D, Kumar Samanta P, Roy S, Adhikary B & Biswas P, *Electrochim Acta*, 144 (2014) 282.

11 Wang J, Wang Z, Zhao D & Xu C, *Anal Chim Acta*, 832 (2014) 34.

12 Wilson R & Turner A P F, *Biosens Bioelectron*, 7 (1992) 165.

13 Zhang L, Li Y, Zhang L, Li D W, Karpuzov D & Long Y T, *Int J Electrochem Sci*, 6 (2011) 819.

14 Zare H R, Nasirizadeh N, Mazloum-Ardakani M & Namazian M, *Sens Actuators B*: *Chem*, 120 (2006) 288.

15 Lates V, Gligor D, Muresan L M & Popescu I C, *J Electroanal Chem*, 661 (2011) 192.

16 Blacker T S, Mann Z F, Gale J E, Ziegler M, Bain A J, Szabadkai G & Duchen M R, *Nat Commun*, 5 (2014) 3936.

17 Zhou Y, Xu Z & Yoon J, *Chem Soc Rev*, 40 (2011) 2222.

18 Ritov V B, Menshikova E V & Kelley D E, *Anal Biochem*, 333 (2004) 27.

19 Omar F S, Duraisamy N, Ramesh K & Ramesh S, *Biosens Bioelectron*, 79 (2016) 763.

20 Sahin M & Ayranci E, *Electrochim Acta*, 166 (2015) 261.

21 Gómez-Anquela C, Revenga-Parra M, Abad J M, García Marín A, Pau J L, Pariente F, Piqueras J & Lorenzo E, *Electrochim Acta*, 116 (2014) 59.

22 Paulus G L C, Wang Q H & Strano M S, *Acc Chem Res*, 46 (2013) 160.

23 Ensafi A A, Ahmadi Z, Jafari-Asl M & Rezaei B, *Electrochim Acta*, 173 (2015) 619.

24 Babaei A, Sohrabi M & Taheri A, *J Electroanal Chem*, 698 (2013) 45.

25 Lin K C, Huang J Y & Chen S M, *RSC Adv*, 3 (2013) 25727.

26 Wooten M & Gorski W, *Anal Chem*, 82 (2010) 1299.

27 Chen Ch-H, Chen Y-C & Lin M-Sh, *Biosens Bioelectron*, 42 (2013) 379.

28 Aydogdu G, Zeybek DK, Zeybek B & Pekyardimci S, *J Appl Electrochem*, 43 (2013) 523.